Dewetting of Stable Thin Polymer Films Induced by a Poor Solvent: Role of Polar Interactions

3 AUTHORS, INCLUDING:

Lin Xu
University of Minho
**15** PUBLICATIONS   **136** CITATIONS

SEE PROFILE

Ashutosh Sharma IITK
Indian Institute of Technology Kanpur
335 PUBLICATIONS   **7,410** CITATIONS

SEE PROFILE

Dewetting of Stable Thin Polymer Films Induced by a Poor Solvent: Role of Polar Interactions

Lin Xu,[†] Ashutosh Sharma,*[,†,‡] and Sang Woo Joo*[,†]

[†]School of Mechanical Engineering, Yeungnam University, Gyongsan 712-749, Korea
[‡]Department of Chemical Engineering, Indian Institute of Technology, Kanpur 208016, India
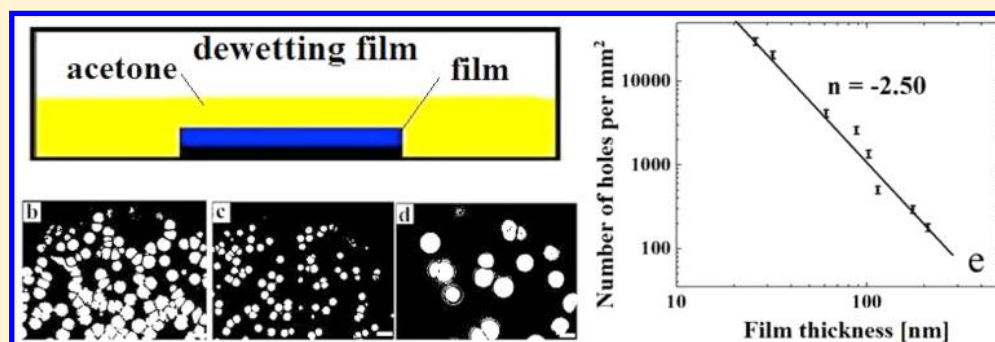
ABSTRACT: We investigate the room temperature instability and dewetting of ultrathin (<100 nm) stable polystyrene (PS) films induced by a poor solvent, such as acetone, on a higher energy silicon substrate without an oxide layer. Instability behavior is contrasted for thermal annealing and acetone-vapor annealing and by immersion under liquid acetone. The PS films that are stable under thermal annealing are rendered unstable to dewetting when contacted by acetone, notwithstanding the stabilizing apolar van der Waals interactions in all the three systems. Relatively high molecular weight films dewet only in the liquid acetone, but low molecular weight films dewet on contact with both vapor and liquid acetone. These findings indicate the role of polar interactions engendered by acetone in the film instability modified possibly by nanophase separation aided by the substrate and nucleative mechanisms. Liquid acetone greatly enhances the instability so that the number density of holes produced in liquid acetone is about 2 orders higher than in acetone vapor. In both of these cases, the scaling ($N \sim H^n$) of the number of holes per unit area, N, with the film thickness, H, is found to be clearly different ($n \sim 2.5$–2.7) from that seen in most of the previous studies on thermal dewetting ($n \sim 4$). From the kinetics of hole growth, the slippage effect of PS chains can be observed in the solvent vapor-induced dewetting process but not in the dewetting under liquid acetone.

1. INTRODUCTION

Ultrathin (<100 nm) polymer films on solid substrates have attracted considerable attention owing to interesting behavior of highly confined soft matter and their numerous technological applications including functional coatings, sensors, multilayer adsorption, patterns on solar panels, fuel cell electrodes, smart adhesives, optoelectronic devices, biological membranes, micro/nano fluidic devices, and drug delivery modules.[1−5] The instability frequently manifests in spontaneous dewetting by the formation of holes, which subsequently grow and coalesce, leading structures with a characteristic length scale.[6−15] Dewetting of thin polymer film also provides an effective pathway to self-organize ultrathin polymer films to fabricate ordered micro/nano polymer structures.[16−22] However, growth of surface instability in air by thermal or solvent vapor annealing is opposed by a strong surface tension effect which increases the length scale of structures. Miniaturization of the instability length scale to smaller sizes remains a major challenge.

In thermally induced spinodal dewetting, film thickness and the effective Hamaker constant of film are the important parameters that influence the characteristic length scale of the instability. For a layered three-component system, the effective Hamaker constant (substrate-1, film-2, bounding medium-3) can be expressed in terms of van der Waals component of each surface tension as[23]

$$A_{123} = (\sqrt{A_{11}} - \sqrt{A_{22}})(\sqrt{A_{33}} - \sqrt{A_{22}})$$
$$= 24\pi d_0{}^2 (\sqrt{\gamma_1^{LW}} - \sqrt{\gamma_2^{LW}})(\sqrt{\gamma_3^{LW}} - \sqrt{\gamma_2^{LW}})$$

where d_0 is a characteristic van der Waals cutoff length, with a best fit value of 0.158 nm.[23]

A positive value of A_{123} indicates a spinodally unstable film. For thermal dewetting in air or vapor, the dispersion component of the medium 3 is zero. Thus, the films without strong residual stresses[24,25] are stable on the higher energy apolar substrates such as Si without an oxide coating ($A_{11} > A_{22}$), which is the case we consider here.

Recently, there are several studies[26−31] on the solvent vapor-induced dewetting of thin films, which is similar to the thermal dewetting process in that the solvent annealing reduces the glass transition temperature to below the room temperature. However, these studies have focused on undulations of the rims of the growing holes rather than on the length scale of the instability by which the holes are produced. However, it is the quantification and minimization of the length scale of instability which are of primary concerns in the formation of ordered microstructures by directed dewetting on physicochemically patterned templates.[32−36]

Recently, dewetting of unstable films has also been studied under a liquid mixture of a good solvent (methyl ethyl ketone) and a nonsolvent (water) that are made compatible to form a homogeneous mixture by addition of a poor solvent such as acetone.[36−38] Dewetting under such a liquid mix allows penetration of good solvent molecules in the film prevents dissolution of the polymer because of the presence of nonsolvent (water) and reduces the polymer interfacial tension by about 2 orders, thus promoting faster and finer dewetting.[36−38] Further, it also changes the destabilizing force for dewetting,[36−39] which appears to be of an electrostatic origin rather than the weaker van der Waals force. Interestingly, even under deserted water,[39] which is a nonsolvent, polymer surfaces can acquire sufficient mobility and are rendered unstable to form a surface nanopattern.[39,40]

Thus, dewetting under suitable liquids can be an effective measure for addressing the problem of miniaturization of structures produced by dewetting. The liquid solvent-induced dewetting may allow greater flexibility in the control of the interfacial tension and effective destabilizing forces by the choice of different solvents. Here we show that a thin polymer film exposed to a poor solvent can be an effective means of destabilizing an otherwise stable film by introduction of destabilizing polar interactions and at the same time intensifying the instability to produce finer dewetted structures compared to vapor annealing. We study the dewetting of a thin polystyrene polymer film on a higher energy apolar Si substrate without an oxide layer, which renders it stable against thermal dewetting by immersing it under a poor liquid solvent, acetone, or its vapor at room temperature. Dewetting is engendered by the introduction of polar interactions despite a stabilizing van der Waals interaction. Use of a poor solvent prevents a rapid dissolution of the polymer during its dewetting while at the same time reduces the glass transition of the polymer, thus rendering it mobile for reorganization. Also, the stabilizing influence of interfacial tension can be significantly reduced, and the Hamaker constant and spreading coefficient of the film can be altered by the choice of the liquid solvent. This further widens the application of dewetting in self-organization of ultrathin polymer films.

On a higher energy Si wafer without the oxide layer, PS film remains stable under thermal annealing in air owing to a positive spreading coefficient and a negative Hamaker constant. During the two dewetting processes in liquid acetone and its vapor, the van der Waals forces continue to play a stabilizing role, but the polar interactions introduced by acetone lead to the instability of the film.

Figure 1 shows the experimental setup of the dewetting in the organic solvent and the solvent vapor-induced dewetting process. For the sake of brevity, we will refer to acetone as the solvent used, while noting that it is actually a poor solvent for the polymer used but interacts more strongly with the Si
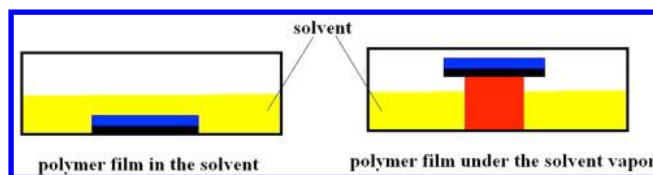

Figure 1. Schematic diagram of the experimental setups.

surface. In both the dewetting processes, the number of holes per unit area decreases with the increase in film thickness. Further, we show that the scaling between the number of holes per unit area and the film thickness is different from most of the previous studies on thermal dewetting of films destabilized by the van der Waals attraction. In all the cases, we also focus on the kinetics of hole growth, which provides important clues regarding the presence or absence of slippage of polymer chains in the two systems. Interestingly, slippage was observed in the solvent vapor-induced dewetting process but was absent in the dewetting process in the liquid organic solvent.

2. EXPERIMENTAL SECTION

As shown in Figure 1, thin PS films were placed in acetone or in saturated acetone vapor at room temperature. Polystyrene (M_w = 97 kg/mol, M_w/M_n = 1.01 and M_w = 390 kg/mol, M_w/M_n = 1.1) was dissolved in toluene and spin-coated onto the Si wafers without the oxide layer. The native oxide layer was removed by hydrofluoric acid. Prior to spin-coating, the wafers were cleaned with deionized water and acetone, then boiled to a 2/1 (v/v) solution of 98% H_2SO_4/30% H_2O_2 for 30 min, and thoroughly rinsed with deionized water and dried with compressed nitrogen. The film thickness was measured by ellipsometry. The residual solvent was removed by treatment in a vacuum oven for 48 h at room temperature. The change of the PS film morphology was observed with an optical microscope (OM) in reflection mode with a CCD camera attachment.

3. RESULTS AND DISCUSSION

A schematic diagram of the experimental setup is shown in Figure 1. During the dewetting process of thin polymer film in liquid acetone, acetone molecules readily diffuse into the PS film and fully saturate it. The high-molecular-weight PS used does not dissolve appreciably during the experiments. Thus, one can think of PS film as a solution of acetone in the polymer. Owing to the presence of acetone in the PS film, the glass transition temperature of the PS is decreased below the room temperature, and the PS chains can glide over one another at the room temperature. In the solvent vapor-induced dewetting process, the quantity of acetone entering into the polymer film is gradual and far less than that in the dewetting process of thin polymer film in liquid acetone. This is one of the factors leading to differences between the two dewetting processes as discussed below. The most important factor, however, is the interfacial tension of the polymer, which is greatly reduced upon contact with liquid acetone.

First, we analyze the number density of holes formed to compare to the two dewetting processes. Figure 2 shows a series of OM images of the PS films (M_w = 390 kg/mol) with different thickness immersed in liquid acetone and the plot of the maximum number of holes per unit area with the film thickness. SEM/EDX showed a clear silicon signal in the dewetted regions, thus confirming the exposure of silicon substrate to acetone in dewetting. Figure 2 shows that the number of holes per unit area decreases with the increase in the film thickness and the decline fits well on a log−log plot. Most of the previous studies on thermal dewetting have reported that
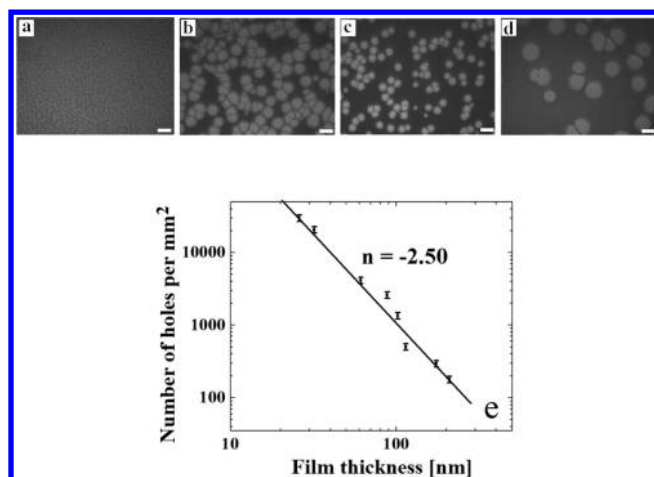
Figure 2. (a−d) A series of OM images of PS (M_w = 390 kg/mol) films with different film thickness on the Si wafer without an oxide layer immersed in liquid acetone at room temperature: (a) h = 26 nm, t = 3 min; (b) h = 61 nm, t = 6 min; (c) h = 102 nm, t = 20 min; (d) h = 174 nm, t = 25 min. The size of the bar is 25 μm. (e) Plot of the number of holes per mm^2 and film thickness. t is the annealing time in liquid acetone.

the number of holes per unit area, N, displayed the scaling $N \sim h^{-4}$, where h is the film thickness.[41,42] However, from Figure 2e, the scaling of the number of holes per unit area and the film thickness is quite different from that in most of the previous studies on thermal dewetting. This implies that the dewetting mechanism is different from that of thermal dewetting or dewetting by a good solvent vapor such as toluene.[26−28] The continued coalescence of holes finally leads to the formation of PS droplets (not shown) as known in thermal annealing.[6,7,41,42] The droplet size did not change even after 2 h of immersion in liquid acetone whereas initiation of dewetting and hole formation were completed within minutes, thus ruling out any significant dissolution.

Unlike the case of dewetting in liquid acetone, when the PS films (M_w = 390 kg/mol) were treated by acetone vapor, it was found that the high molecular weight PS films were still stable after 24 h. Thus, a much smaller quantity of the acetone entering in the PS film from the vapor phase is evidently not sufficient to induce enough chain mobility, and the glassy state with its residual elasticity is still maintained in the high molecular weight films despite relatively long vapor exposures. Such weakly elastic films once ruptured to attain a contact line can dewet by further contact line movement[43] but are not spontaneously unstable to initiation of dewetting.[44] However, the lower molecular weight films dewetted readily by acetone vapor exposure.

Figure 3 shows a series of OM images of the PS film (M_w = 97 kg/mol) morphology with different thickness in acetone vapor and the plot of the number of holes per unit area and the film thickness. As in the case of liquid acetone dewetting, the number of holes per unit area decreases with the increase in film thickness. However, as also noted earlier, the scaling of the number of holes per unit area with the film thickness is again different from the previous studies on the thermal dewetting.[6,7,41,42] Interestingly, although the exponents n in $N \sim h^{-n}$ are similar for liquid and vapor acetone dewetting (n = 2.5 and 2.77, respectively), the hole density is more than an order of magnitude higher in liquid acetone compared to acetone vapor. Except for one thickness (∼25 nm film where the ratio is ∼20),
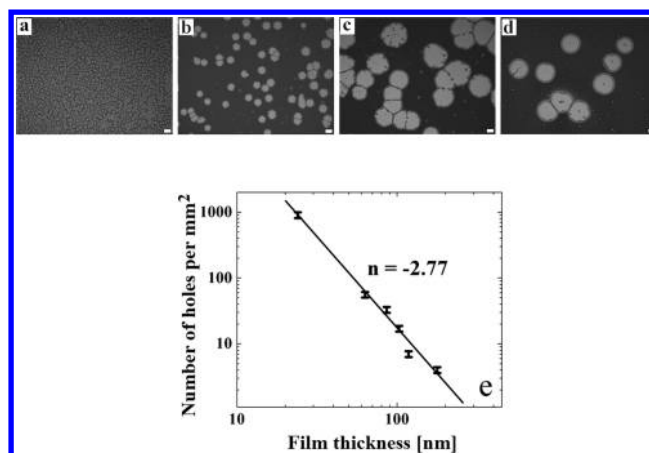

Figure 3. (a−d) A series of OM images of PS (M_w = 97 kg/mol) films with different film thickness on the Si wafer without oxide layer annealed in acetone vapor at room temperature: (a) h = 24 nm, t = 1 h; (b) h = 63 nm, t = 5 h; (c) h = 103 nm, t = 6 h; (d) h = 118 nm, t = 6 h. The size of the bar is 50 μm. (e) Plot of the number of holes per mm^2 and film thickness. t is the annealing time in acetone vapor.

the ratio of hole densities is in a narrow range of 70−80 for all other thicknesses. Further, the time scale for the formation of holes is reduced by more than 1 order in liquid acetone compared to vapor annealing.

The insets in Figure 4 show the radial average of 2-D Fourier transform. The presence of the peak implies that the positions
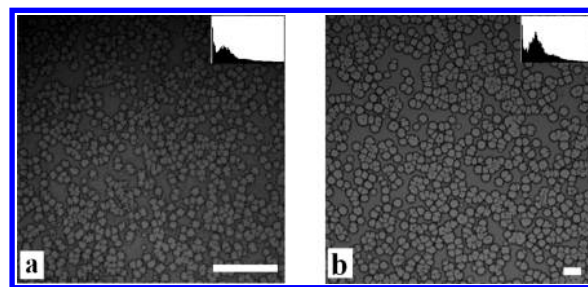

Figure 4. (a) OM image of a PS film (M_w = 390 kg/mol, h = 26 nm) under liquid acetone at room temperature. (b) OM images of PS films (M_w = 97 kg/mol, h = 24 nm) annealed by acetone vapor at room temperature. The size of the bars is 50 μm. The insets in are the radial average of 2-D Fourier transform.

of holes are correlative and the position of the peak determines the characteristic wavelength of the instability. The wavelength in Figure 4a ($\lambda \sim$ 7 μm) under liquid acetone is obviously smaller than that obtained by vapor annealing in Figure 4b ($\lambda \sim$ 30 μm).

We also investigated the kinetics of hole growth in the two dewetting processes. Figure 5 shows the kinetics of hole growth in the dewetting of high molecular weight PS (M_w = 390 kg/mol) film in liquid acetone. From Figure 5, it is seen that the radii of holes increases almost linearly with time during the hole growth. This implies that the slippage effect of polymer chains is absent in the dewetting process,[45,46] indicating their adequate disentanglement in liquid acetone. In contrast, Figure 6 shows the kinetics of holes growth in the solvent vapor-induced dewetting of a lower molecular weight PS (M_w = 97 kg/mol) film. From Figure 6, the slippage effect is observed in the kinetics of holes growth as the exponent m ($R \sim t^m$) is in the range 0.56−0.58, which is close to its theoretical value of 2/3
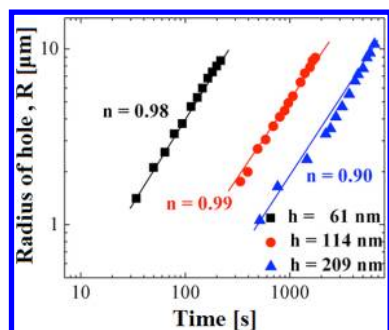
Figure 5. Radius of hole with time in the dewetting process of PS (M_w = 390 kg/mol) film under liquid acetone at room temperature.
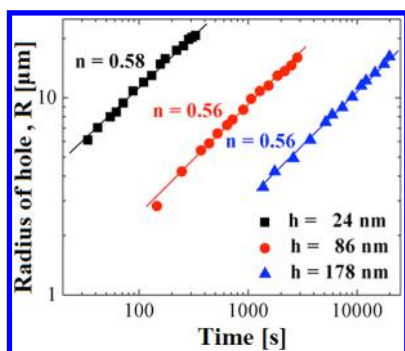

Figure 6. Radius of hole and time in the dewetting process of PS (M_w = 97 kg/mol) film annealed by acetone vapor at room temperature.

for the hole-growth with strong slip.[45−47] From the results in Figures 5 and 6, there is a great difference between the two dewetting processes in the kinetics of the hole growth. Clearly, the absence of slippage under liquid solvent annealing (Figure 5) and strong slippage under acetone vapor annealing (Figure 6) cannot be explained by the different molecular weight of the films used in the two processes. On the contrary, the high molecular weight used in liquid annealing (M_w = 390 kg/mol) should encourage slip because of the stronger chain entanglement and the low molecular weight (M_w = 97 kg/mol) used in the vapor annealing should promote no-slip. However, we observe the opposite of the results anticipated from the effect of molecular weight on slippage. Thus, one has to examine the possible differential effects of the solvent vapor versus liquid annealing. The slippage indicated under acetone vapor may result from two factors: persistence of partial chain entanglement and possibility of nanophase separation[48] in the film including the formation of a thin layer of low viscosity acetone at the Si−polymer interface owing to substrate induced phase separation because of the greater affinity of acetone for the substrate. Indeed, acetone almost completely wets the Si surface (the measured contact angle of acetone on the Si wafer was 3 ± 1°), whereas the contact angle of acetone laden PS is about 20°.[27] A very low viscosity underlayer compared to the polymer film results in slippage.[49,50]

The slippage is characterized by the slip length b, which is defined as the distance from the wall at which the velocity extrapolates to zero. For the simple liquids, $b \sim a$, where a is a molecular size. However, b can be large for the polymer chains where $b \sim N^3/N_e^2$, where N is the index of polymerization and N_e is the threshold for entanglement. Polymer chains entanglement is an important factor leading to slippage. The polymer chains with higher molecular weight have stronger

chain entanglement inducing stronger slip. In addition, acetone molecules can form an ultrathin layer at the silicon substrate. The lubricating influence of the low viscosity underlayer can result in a strong slip of the high viscosity polymer film owing to low shear force at the polymer−substrate boundary. Theoretically, in the case of strong slip, the capillary driving force, S, for the hole growth per unit length of the rim is balanced by the resisting friction force.[45] This leads to the well-known kinetics of the hole growth for slipping films: $R \sim t^{2/3}$.[45]

In the following, we discuss the mechanism of hole formation in the solvent, which requires a brief connection with the theory of thin film stability.[28,32,33,41,51−53] For a thin apolar polymer film (polystyrene), the effective Hamaker constant of film is the main parameter influencing the stability of thin film. However, when the polar solvent molecules enter into the PS film, the polar interactions have to be considered. For thin film system under consideration, the total excess free energy per unit area can be expressed as the sum of apolar van der Waals (ΔG^{LW}) and the polar acid−base (ΔG^{AB}) interaction energies[23,32,33,51−54]

$$\Delta G = \Delta G^{LW} + \Delta G^{AB} = -A_{123}/12\pi h^2 + S^P f(h) \quad (1)$$

where h is the film thickness, A_{123} is the effective Hamaker constant (substrate-1, film-2, medium-3) related to the apolar spreading coefficient by $A_{123} = -12\pi d_0^2 S^{LW}$, and S^P is the polar component of spreading coefficient. The apolar and polar components of spreading coefficients are defined in turn by the apolar (LW) and the polar (AB) components of surface and interfacial tensions (substrate-1, film-2, bounding medium-3): $S^{LW} = \gamma_{13}^{LW} - \gamma_{12}^{LW} - \gamma_{23}^{LW}$ and $S^{AB} = \gamma_{13}^{AB} - \gamma_{12}^{AB} - \gamma_{23}^{AB}$. By definition, the decay function for the polar interactions, $f(h)$, satisfies the relations $f(h) = 1$ at the cutoff d_0 and $f(h) = 0$ at large distances. The polar AB interactions often decay exponentially for simple liquids,[23] but their decay behavior for the polymer−solvent mixtures is not known. The correlation length for the decay is likely to be of the order of the radius of gyration for the polymer in the solvent.

The spinodal instability of a thin film requires that the spinodal parameter should be negative, i.e., the condition $\partial^2 \Delta G/\partial h^2 < 0$. The number density of holes for an unstable film is given by

$$N = \lambda^{-2} = [-(\partial^2 \Delta G/\partial h^2)/8\pi^2 \gamma_{23}] \quad (2)$$

where λ is the dominant length scale of the instability. For a purely apolar van der Waals potential, instability occurs only when the effective Hamaker constant is positive, $A_{123} > 0$, or in other words the apolar spreading coefficient S^{LW} is negative, signifying promotion of nonwettability by the van der Waals force.

For the films under liquid acetone, the effective Hamaker constant can be expressed in terms of the LW component of each surface tension:[14,27,41]

$$A_{123} = (\sqrt{A_{11}} - \sqrt{A_{22}})(\sqrt{A_{33}} - \sqrt{A_{22}})$$
$$= 24\pi d_0^2(\sqrt{\gamma_1^{LW}} - \sqrt{\gamma_2^{LW}})(\sqrt{\gamma_3^{LW}} - \sqrt{\gamma_2^{LW}}) \quad (3)$$

where d_0 is the van der Waals cutoff length (∼0.158 nm). The medium phase (3) is either vapor ($\gamma_3^{LW} = 0$) or liquid acetone ($\gamma_3^{LW} = 18$ mN/m; $\gamma_3 = 23.3-25.2$ mN/m).[55] Further, the polar component of the spreading coefficient can be calculated from

$$S = S^{LW} + S^P = \gamma_{23}(\cos\theta - 1) \qquad (4)$$

where the dispersion component $S^{LW} = -A_{123}/12\pi d_0^2$.

A further complexity in the above description is the role of heterogeneities or "nucleation", which becomes increasingly important for the relatively thicker films studied here.[32,33,53] However, as a rough guide, the ratio of heterogeneous to spinodal length scales is given by[32,33,53]

$$\lambda_h/\lambda \sim [1 + \Delta\varphi/(-\varepsilon c(\partial^2\Delta G/\partial h^2))]^{-1/2}$$

where $\Delta\varphi$ is the potential difference created by the heterogeneity at mean film thickness h. Here ε ($<h$) and c (<1) depend on the details of the initial conditions and the heterogeneity, respectively, and the parameter $(\partial^2\Delta G/\partial h^2)$ in the above equation is now evaluated for the heterogeneous sites. An implication is that the stabilizing role of surface tension and thus its influence on the length scale remains unchanged, but the dependence of λ on the film thickness can be altered when heterogeneous mechanism becomes dominant, $\Delta\varphi/(-\varepsilon c(\partial^2\Delta G/\partial h^2)) \gtrsim 1$). The length scale can also be altered by nanophase separation of the poor solvent in the film.[48] Finally, a further complexity is alteration of instability length scale by strong slippage.[56] These complexities together with the unknown decay of the polar interactions, $f(h)$, precludes the possibility of an a priori theoretical prediction of $\lambda(h)$ presently, but they point to some important directions for the future work.

Applying eq 3 to the system of the PS film on the Si wafer without the oxide layer in air (γ_1^{LW} = 35.6 mN/m, γ_2^{LW} = 28.3 mN/m, and γ_3^{LW} = 0) yields the effective Hamaker constant of the system, A_{123} = -6.72×10^{-21} J < 0. Basically for any $\gamma_1^{LW} > \gamma_2^{LW}$, the van der Waals force is stabilizing. Indeed, these films do not dewet by thermal annealing. When polar acetone molecules enter the PS film, we have to take the polar interactions into consideration in the stability of thin films. During the dewetting of PS film in acetone vapor, the effective Hamaker constant of the solvent-laden film should be even more negative because the apolar part of the surface tension of acetone ($\gamma^{LW}_{acetone}$ = 18 mN/m; total $\gamma_{acetone}$ = 23.3–25.2 mN/m)[27,55] is smaller than that of PS (γ_2^{LW} = 28.3 mN/m). On the basis of some approximations, Lee et al. computed the Hamaker constant of PS film under acetone vapor to be -1.65×10^{-20} J and the polar component of the spreading coefficient, S^P, to be -18.95 mN/m.[27] Thus, the instability and nonwettability of the film in acetone vapor are induced by the polar interactions as announced by the eqs 1 and 4.

While it is not possible to quantify the magnitude of the (negative) polar spreading coefficient of PS films under liquid acetone because of the lack of information on the acid–base interactions of acetone with wafer and PS, two differences from the acetone vapor case are clear. Considering eq 3, we deduce that the three phase effective Hamaker constant of the PS film fully saturated with acetone ($\gamma_2^{LW} \sim \gamma^{LW}_{acetone}$ = 18 mN/m) and immersed in the bulk liquid acetone ($\gamma_3^{LW} = \gamma^{LW}_{acetone}$ = 18 mN/m) should be close to zero, and in any case much smaller than the acetone-laden PS film in acetone vapor, where γ_3^{LW} = 0. Thus, the stabilizing van der Waals interaction under liquid acetone is far weaker. Even more important is a substantial reduction in the interfacial tension of PS under liquid acetone, which, according to eq 2, can greatly reduce the length scale of instability. The minimum value of the total surface tension γ_2 of PS in acetone vapor is $\gamma_2 \sim \gamma_{acetone} \sim 24$ mN/m, and the maximum value is $\gamma^{LW}_{PS} \sim 35$ mN/m. The PS–acetone mixture

surface tension should be between these two limits. On replacing the vapor by liquid, the surface tension γ_2 is replaced by a much smaller interfacial tension, $\gamma_{23} = [(\gamma_2^{LW})^{1/2} - (\gamma_2^{LW})^{1/2}]^2$ plus a polar component which cannot be estimated, but should be much smaller owing to acetone being a polar solvent for PS and the PS film being completely saturated by acetone. This indicates the interfacial tension in the range of near zero to a maximum value of ~ 1 mN/m even by assuming the PS to be pure (without any acetone penetration; $\gamma_2^{LW} \sim 28.3$ mN/m). Thus, about 2 orders of magnitude reduction in the PS–solvent interfacial tension is indicated under liquid acetone. Thus, it appears that the increase in the hole density under liquid acetone by a factor of 70–80 can be explained mostly by a similar reduction in surface tension and to a more minor extent by the removal of stabilizing van der Waals force under liquid acetone ($A = -1.65 \times 10^{-20}$ J is substantial and negative under acetone vapor but nearly zero under acetone liquid).

4. CONCLUSIONS

Thermally annealed thin polymer films that are stable on higher energy substrates owing to stabilizing repulsive van der Waals force can be made unstable at room temperature by contact with vapor of a poor solvent and, to a much greater extent, by immersing them in the same liquid solvent. The presence of acetone in PS film decreases the glass transition temperature below the room temperature. The instability is induced in these cases by the attractive polar interactions that engender a negative component of the polar spreading coefficient and thus a finite three-phase contact angle as evidenced by the formation and growth of holes. It thus appears attractive to explore this method for the structure formation in thin composite polymer films that are otherwise rendered stable to thermal annealing by other means, such as by the addition of nanoparticles.[57−64]

There are, however, major differences between the instability engendered by the solvent vapor and liquid. For high molecular weight PS films (e.g., M_w = 390 kg/mol), the motion of polymer chains remains arrested under acetone vapor because of a small quantity of solvent molecules that penetrate limited both by kinetics and solubility. Such films remain at least kinetically stable under vapor but rupture readily under liquid solvent. When rupture does occur under vapor contact, the growth kinetics of holes shows a signature of slippage, which is absent under liquid solvent. This may be due to a strong substrate−solvent interaction mediated formation of a thin acetone layer of low viscosity under the slipping polymer mass of much higher viscosity. Such substrate-induced nanophase separation becomes less likely when the polymer is fully saturated and surrounded by liquid acetone, which also fills the expanding hole.

The most interesting feature is between 1 and 2 orders of magnitude increase in the density of microstructures produced by the instability and a similar reduction in the time scale in the liquid solvent compared to its vapor. The major reason is more than an order of magnitude reduction in the stabilizing interfacial tension under the liquid solvent. A minor reason is the removal of the stabilizing van der Waals force, which in fact becomes even more prominent in vapor annealing compared to thermal annealing. These features are especially attractive in the creation and miniaturization of self-organized ordered micro/nano polymer structures by directed dewetting of thin films.[16−22,34,35]

■ AUTHOR INFORMATION

Corresponding Author

*E-mail: ashutos@iitk.ac.in (A.S.); swjoo@yu.ac.kr (S.W.J.).

Notes

The authors declare no competing financial interest.

■ REFERENCES

(1) Kim, S. H.; Misner, M. J.; Russell, T. P. *Adv. Mater.* **2004**, *16*, 2119−2123.

(2) Manigandan, S.; Majumder, S.; Suresh, A.; Ganguly, S.; Kargupta, K.; Banerjee, D. *Sens. Actuators, B* **2010**, *144*, 170−175.

(3) Yoneda, H.; Nishimura, Y.; Doi, Y.; Fukuda, M.; Kohno, M. *Polym. J.* **2010**, *42*, 425−437.

(4) Nakata, K.; Kobayashi, T.; Tokunaga, E. *Opt. Rev.* **2010**, *17*, 346−351.

(5) Wang, X.; Yakovlev, S.; Beers, K. M.; Park, M. J.; Mullin, S. A.; Downing, K. H.; Balsara, N. N. *Macromolecules* **2010**, *43*, 5306−5314.

(6) Becker, J.; Grün, G.; Seemann, R.; Mantz, H.; Jacobs, K.; Mecke, K.; Blossey, A. *Nat. Mater.* **2003**, *2*, 59−63.

(7) Gabriele, S.; Sclavons, S.; Reiter, G.; Damman, P. *Phys. Rev. Lett.* **2006**, *96*, 156105.

(8) Karapanagiotis, I.; Gerberich, W. W. *Surf. Sci.* **2005**, *594*, 192−202.

(9) Yoon, B. K.; Huh, J.; Kim, H.-C.; Hong, J.-M.; Park, C. *Macromolecules* **2006**, *39*, 901−903.

(10) Gabriele, S.; Damman, P.; Sclavons, S.; Desprez, S.; Coppée, S.; Reiter, G.; Hamieh, M.; Akhrass, S. A.; Vilmin, T.; Raphaël, E. *J. Polym. Sci., Part B: Polym. Phys.* **2006**, *44*, 3022−3030.

(11) Pototsky, A.; Bestehorn, M.; Merkt, D.; Thiele, U. *J. Chem. Phys.* **2005**, *122*, 224711.

(12) de Silva, J. P.; Geoghegan, M.; Higgins, A. M.; Krausch, G.; David, M.-O.; Reiter, G. *Phys. Rev. Lett.* **2007**, *98*, 267802.

(13) Verma, R.; Sharma, A. *Ind. Eng. Chem. Res.* **2007**, *46*, 3108−3118.

(14) Xu, L.; Yu, X. F.; Shi, T. F.; An, L. J. *Macromolecules* **2008**, *41*, 21−24.

(15) Lee, J.-M.; Kim, B.-I. *Mater. Sci. Eng., A* **2007**, *449−451*, 769−771.

(16) Besancon, B. M.; Green, P. F. *J. Chem. Phys.* **2007**, *126*, 224903.

(17) Eguilaz, M.; Aguei, L.; Yanez-Sedeno, P.; Pingarron, J. M. *J. Electroanal. Chem.* **2010**, *644*, 30−35.

(18) Ogawa, H.; Kanaya, T.; Nishida, K.; Matsuba, G.; Majewski, J. P.; Watkins, E. *J. Chem. Phys.* **2009**, *131*, 104907.

(19) Neto, C.; James, M.; Telford, A. M. *Macromolecules* **2009**, *42*, 4801−4808.

(20) Chung, H-j.; Ohno, K.; Fukuda, T.; Composto, R. J. *Macromolecules* **2007**, *40*, 384−388.

(21) Bandyopadhyay, D.; Sharma, A. *J. Phys. Chem. B* **2008**, *112*, 11564−11572.

(22) Bandyopadhyay, D.; Sharma, A. *J. Phys. Chem. C* **2010**, *114*, 2237−2247.

(23) van Oss, C. J.; Chaudhury, M. K.; Good, R. J. *Chem. Rev.* **1988**, *88*, 927−941.

(24) Thomas, K. R.; Chenneviere, A.; Reiter, G.; Steiner, U. *Phys. Rev. B* **2011**, *83*, 021804.

(25) Reiter, G.; Hamieh, M.; Damman, P.; Sclavons, S.; Gabriele, S.; Vilmin, T.; Raphael, E. *Nat. Mater.* **2005**, *4*, 754−758.

(26) Xu, L.; Shi, T. F.; Dutta, P. K.; An, L. J. *J. Chem. Phys.* **2007**, *127*, 144704.

(27) Lee, S. H.; Yoo, P. J.; Kwon, S. J.; Lee, H. H. *J. Chem. Phys.* **2004**, *121*, 4346.

(28) Thiele, U.; Mertig, M.; Pompe, W. *Phys. Rev. Lett.* **1998**, *80*, 2869−2872.

(29) Bormashenko, E.; Pogreb, R.; Musin, A.; Stanevsky, O.; Bormashenko, Y.; Whyman, G.; Barkay, Z. *J. Colloid Interface Sci.* **2006**, *300*, 293−297.

(30) Xu, L.; Shi, T. F.; An, L. J. *J. Chem. Phys.* **2008**, *129*, 044904.

(31) Xu, L.; Shi, T. F.; An, L. J. *Langmuir* **2007**, *23*, 9282−9286.

(32) Konnur, R.; Kargupta, K.; Sharma, A. *Phys. Rev. Lett.* **2000**, *84*, 931−934.

(33) Kargupta, K.; Sharma, A. *J. Colloid Interface Sci.* **2002**, *245*, 99−115.

(34) Mukherjee, R.; Bandyopadhyay, D.; Sharma, A. *Soft Matter* **2008**, *4*, 2086−2097.

(35) Mukherjee, R.; Gonuguntla, M.; Sharma, A. *J. Nanosci. Nanotechnol.* **2007**, *7*, 2069−2075.

(36) Verma, A.; Sharma, A. *Soft Matter* **2011**, *7*, 11119−11124.

(37) Verma, A.; Sharma, A. *Macromolecules* **2011**, *44*, 4928−4935.

(38) Verma, A.; Sharma, A. *Adv. Mater.* **2010**, *22*, 5306−5309.

(39) Siretanu, I.; Chapel, J. P.; Drummond, C. *ACS Nano* **2011**, *5*, 2939−2947.

(40) Siretanu, I.; Chapel, J. P.; Drummond, C. *Macromolecules* **2012**, *45*, 1001−1005.

(41) Sharma, A.; Reiter, G. *J. Colloid Interface Sci.* **1996**, *178*, 383−399.

(42) Reiter, G. *Phys. Rev. Lett.* **1992**, *68*, 75−78.

(43) Shenoy, V.; Sharma, A. *Phys. Rev. Lett.* **2002**, *88*, 236101.

(44) Sarkar, J.; Sharma, A. *Langmuir* **2010**, *26*, 8464−8473.

(45) Brochard-Wyart, F.; Debrégeas, G.; Fondecave, R.; Martin, P. *Macromolecules* **1997**, *30*, 1211−1213.

(46) Jacobs, K.; Seemann, R.; Schatz, G.; Herminghaus, S. *Langmuir* **1998**, *14*, 4961−4963.

(47) Reiter, G.; Khanna, R. *Langmuir* **2000**, *16*, 6351−6357.

(48) Sharma, A.; Mittal, A. J.; Verma, R. *Langmuir* **2002**, *18*, 10213−10220.

(49) Xu, L.; Sharma, A.; Joo, S. W. *Macromolecules* **2011**, *44*, 9335−9340.

(50) Xu, L.; Bandyopadhyay, D.; Shi, T. F.; An, L. J.; Sharma, A.; Joo, S. W. *Polymer* **2011**, *52*, 4345−4354.

(51) Sharma, A. *Langmuir* **1993**, *9*, 861−869.

(52) Sharma, A.; Jameel, A. T. *J. Colloid Interface Sci.* **1993**, *161*, 190−208.

(53) Sharma, A. *Eur. Phys. J. E* **2003**, *12*, 397−408.

(54) Reiter, G.; Khanna, R.; Sharma, A. *Phys. Rev. Lett.* **2000**, *85*, 1432−1435.

(55) Koenhen, D. M.; Smolders, C. A. *J. Appl. Polym. Sci.* **1975**, *19*, 1163−1179.

(56) Kajari, K.; Sharma, A.; Khanna, R. *Langmuir* **2004**, *20*, 244−253.

(57) Barnes, K. A.; Karim, A.; Douglas, J. F.; Nakatani, A. I.; Gruell, H.; Amis, E. J. *Macromolecules* **2000**, *33*, 4177−4185.

(58) Mackay, M. E.; Hong, Y.; Jeong, M.; Hong, S.; Russell, T. P.; Hawker, C. J.; Vestberg, R.; Douglas, J. F. *Langmuir* **2002**, *18*, 1877−1882.

(59) Krishnan, R. S.; Mackay, M. E.; Hawker, C. J.; Van Horn, B. *Langmuir* **2005**, *21*, 5770−5776.

(60) Besancon, B. M.; Green, P. F. *J. Chem. Phys.* **2007**, *126*, 224903.

(61) Koo, J.; Shin, K.; Seo, Y.-S.; Koga, T.; Park, S.; Satija, S.; Chen, X.; Yoon, K.; Hsiao, B. S.; Sokolov, J. C.; Rafailovich, M. H. *Macromolecules* **2007**, *40*, 9510−9516.

(62) Holmes, M. A.; Mackay, M. E.; Giunta, R. K. *J. Nanopart. Res.* **2007**, *9*, 753−763.

(63) Sharma, S.; Rafailovich, M. H.; Peiffer, D.; Sokolov, J. *Nano Lett.* **2010**, *1*, 511−514.

(64) Mukherjee, R.; Das, S.; Das, A.; Sharma, S. K.; Raychaudhuri, A. K.; Sharma, A. *ACS Nano* **2010**, *4*, 3709−3724.